Macromolecular Research, Vol. 16, No. 5, pp 404-410 (2008)

Preparation and Characterization of Polypropylene/Waste Ground Rubber Tire Powder Microcellular Composites by Supercritical Carbon Dioxide

Zhen Xiu Zhang, Sung Hyo Lee, and Jin Kuk Kim*

School of Nano and Advanced Materials Engineering, Gyeongsang National University, Gyeongnam, Jinju 660-701, Korea

Shu Ling Zhang

School of Nano and Advanced Materials Engineering, Gyeongsang National University, Gyeongnam, Jinju 660-701, Korea
Alan G. MacDiarmid Lab, College of Chemistry, Jilin University, Changchun, 130012, People's Republic of China

Zhen Xiang Xin

School of Nano and Advanced Materials Engineering, Gyeongsang National University, Gyeongnam, Jinju 660-701, Korea
Key Laboratory of Rubber-Plastics (QUST) of Ministry of Education, Qingdao University of Science and Technology, Qingdao, 266042, People's Republic of China

Received September 9, 2007; Revised January 31, 2008; Accepted February 1, 2008

Abstract: In order to obtain 'value added products' from polypropylene (PP)/waste ground rubber tire powder (WGRT) composites, PP/WGRT microcellular foams were prepared via supercritical carbon dioxide. The effects of blend composition and processing condition on the cell size, cell density and relative density of PP/WGRT microcellular composites were studied. The results indicated that the microcellular structure was dependent on blend composition and processing condition. An increased content of waste ground rubber tire powder (WGRT) and maleic anhydride-grafted styrene-ethylene-butylene-styrene (SEBS-*g*-MA) reduced the cell size, and raised the cell density and relative density, whereas a higher saturation pressure increased the cell size, and reduced the cell density and relative density. With increasing saturation temperature, the cell size increased and the relative density decreased, whereas the cell density initially increased and then decreased.

Keywords: microcellular composites, morphology, recycling, waste ground rubber tire powder, supercritical carbon dioxide.

Introduction

The foamed polymers exhibit many advantages over the unfoamed polymers such as higher impact strength, higher toughness, higher stiffness-to-weight ratio, higher fatigue life, higher thermal stability, lower dielectric constant, and lower thermal conductivity.[1-4] Therefore they could be applied to many fields like food packaging, airplane and automotive parts, sporting equipment, insulation, controlled release devices and filter.[1,5,6] A pressure-quench method described by Goel and Beckman[7] is widely used for making microcellular polymers via supercritical carbon dioxide. Unlike the previous batch process invented by Martini and coworkers,[8] the pressure-quench method takes advantage of the plasticization effect of polymers by CO_2 swelling. The glass-transition temperature (T_g) of CO_2-saturated polymers could be depressed to room temperature.[9] Therefore, Goel and Beckman[7] found that the microcellular structure could be achieved by rapid depressurization rather than increasing the temperature above the T_g of pure polymers to allow the microcells nucleation and growth.

Due to its outstanding characteristics and low cost, polypropylene (PP) has been considered as a substitute for other thermoplastic foam materials.[10] But it does not provide a high enough state of physical properties at a given flexibility to fully compete in the cellular elastomer market.[11] To improve the impact toughness and extend its application range, a number of studies on toughening PP with rubber have been made in the last 20 years and thoroughly reviewed by Liang and Li.[12-14] Recycling of waste ground rubber tire powder is our preference from the ecological and economical point of view. The usage of WGRT as dispersed phase in PP matrix offers an interesting opportunity for recycling of WGRT. PP/WGRT composites show the simi-

*Corresponding Author. E-mail: rubber@gsnu.ac.kr

lar performance and processing characteristics to thermoplastic vulcanizates (TPV), therefore can be regarded as thermoplastic elastomers. The TPV foaming technology is to fulfill the requirement of lower cost, lighter weight and better fuel economy, therefore presents an important milestone in many applications.

Our laboratory has been focusing considerable attention on the development of thermoplastic vulcanizates from waste ground rubber tires.[15] The present work is continuation of our research efforts to obtain 'value added products' from PP/WGRT composites, namely deals with the production of microcellular composites from the same by $scCO_2$. And the effect of the blend composition and processing condition on the microcellular structure of PP/WGRT microcellular composites is reported.

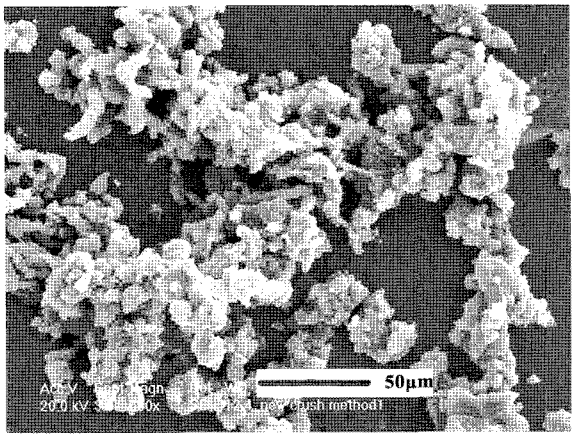

Figure 1. SEM microphotograph of 30-40 μm waste ground rubber tire powder.

Experimental

Materials and Sample Preparation. Polypropylene (Co-PP, B391M) was manufactured by SK Corporation. Maleic anhydride-grafted styrene-ethylene butylene-styrene (SEBS-*g*-MA, Kraton FG-1901X) was obtained from Shell Chemical Co. Ltd. Waste ground rubber tire powder was produced by wet grinding method and its particle size was characterized to be 30-40 μm as shown in Figure 1. CO_2 with a purity of 99.95% was supplied by Hyundai Gas Inc.

Composites were prepared using an internal mixer. The blend composition is given in Table I. The mixing conditions were 180 °C, 60 rpm, and 10 min. After mixing, the plate samples of the composites with 3.0 mm thickness were compression-molding at 180 °C for 6 min.

Foam Preparation. The foams were prepared using a pressure-quench method described by Goel and Beckman.[7] Plate samples that were 3.0 mm thick, 20.0 mm long, and 4.0 mm wide were enclosed high-pressure vessel. The vessel was flushed with low-pressure CO_2 for about 3 min and pressurized to the saturated vapor pressure CO_2 at room temperature and preheated to desired temperature. Afterward, the pressure was increased to the desired pressure by a syringe pump (ISCO260D) and maintained at this pressure for 3 h to ensure equilibrium absorption of CO_2 by the samples. After saturation, the pressure was quenched atmospheric pressure within 3 s and the samples were taken out. Then foam structure was allowed to full growth during rapid depressurization. The processing condition is listed in Table II.

Foam Characterization. The foamed samples were fractured in liquid nitrogen, coated with an approximately 10-nm thick layer of gold on the fractured surface, and observed with a Philips XL 30S scanning electron microscope (SEM). The cell sizes, cell densities and relative densities were characterized. The cell diameter (D) is the average of all the cells on the SEM photo, usually more than 100 cells were measured.

$$D = d/(\pi/4) \quad (1)$$

Where d is the measured average diameter in the micrograph.

The density of foam and unfoamed samples was determined from the sample weight in air and water respectively, according to ASTM D 792 method A. Then the density of

Table I. Blend Composition and Foam Characteristics for Samples

Co-PP (g)	WGRT (g)	SEBS-*g*-MA (g)	Average Cell Size D (μm)	Cell Density N_0 (cells/cm^3)	Relative Density (%)
100	0	0	28.9	3.16×10^8	0.200
80	20	0	22.7	3.35×10^8	0.329
70	30	0	17.8	4.20×10^8	0.445
60	40	0	15.3	5.35×10^8	0.500
50	50	0	13.7	5.93×10^8	0.554
40	60	0	11.3	7.48×10^8	0.640
60	40	5	13.6	6.64×10^8	0.533
60	40	20	8.1	1.63×10^9	0.690

Table II. Processing Condition and Foam Characteristics for Samples

Pressure (MPa)	Temperature (°C)	Co-PP/WGRT (wt%)	Average Cell Size D (μm)	Cell Density N_0 (cells/cm^3)	Relative Density (%)
18	120	100/0	2.2	1.45×10^{10}	0.869
		70/30	2.0	1.14×10^{10}	0.908
18	150	100/0	3.3	1.70×10^{10}	0.764
		70/30	3.1	1.24×10^{10}	0.831
18	160	100/0	4.8	7.21×10^{9}	0.711
		70/30	3.8	8.24×10^{9}	0.803
18	165	100/0	28.9	3.16×10^{8}	0.197
		70/30	17.8	4.19×10^{8}	0.445
14	165	100/0	6.1	6.73×10^{9}	0.562
		70/30	5.2	5.13×10^{9}	0.723
10	165	100/0	3.6	1.15×10^{10}	0.783
		70/30	3.3	6.01×10^{9}	0.900

the foamed sample is divided by the density of the unfoamed sample to obtain the relative density (ρ_r). The volume fraction occupied by the microvoids (V_f) was calculated as

$$V_f = 1 - \frac{\rho_f}{\rho_m} \tag{2}$$

Where ρ_m and ρ_f are the density of the unfoamed polymer and foamed polymer respectively.

The cell density (N_0) based on the unfoamed sample was calculated as

$$N_f = \frac{V_f}{\frac{\pi}{6}D^3} \tag{3}$$

$$N_0 = \frac{N_f}{1 - V_f} \tag{4}$$

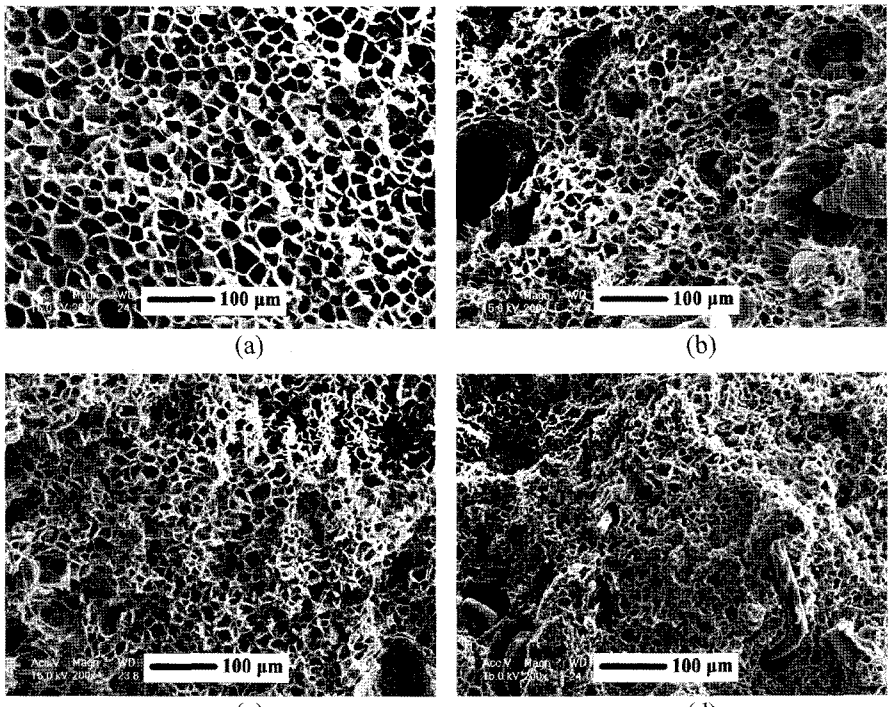

(a) (b) (c) (d)

Figure 2. Effect of WGRT powder loading on microcellular structure of PP/WGRT blends foaming at 18 MPa, 165 °C: (a) PP/WGRT=100/0; (b) PP/WGRT=80/20; (c) PP/WGRT=60/40; (d) PP/WGRT=40/60 (SEM microphotograph).

Where V_f is the volume fraction occupied by the microvoids, N_f is the cell density based on the foamed sample.

Results and Discussion

Effect of Blend Composition on Microcellular Structure.

The WGRT Loading: It is known that the mechanisms of cell nucleation and growth of polymers are influenced by the dissolved amount of CO_2 in polymer, the diffusivity of CO_2 within polymer and the diffused rate of CO_2 from polymer.[16,17] Figure 2 illustrates the effect of the WGRT loading on microcellular structure of PP/WGRT composites and the foam characteristics for samples can be seen in Table I. From Table I, it can be observed that average cell sizes of PP/WGRT composites decrease with increasing the WGRT loading, whereas the corresponding cell densities and relative densities increase. This may be due to the stepwise increase of WGRT causing the gradual increase of heterogeneous nucleation, the melt viscosity and CO_2 diffused rate from PP.[18-20] Namely the increase of WGRT as nucleating agent enhances cell nucleation, whereas the increase of the melt viscosity and CO_2 diffused rate from PP causes more resistance to cell nucleation and growth. Therefore the cell densities of PP/WGRT composites slightly increase with increasing the WGRT loading, whereas the average cell sizes decrease. In addition, since WGRT powder cannot be foamed, the more the amount of WGRT in the sample is, the larger the relative densities of the sample is.

SEBS-*g*-MA Loading: Figure 3 illustrates the effect of SEBS-*g*-MA loading on microcellular structure of PP/WGRT blends and the foam characteristics for samples can be seen in Table I. From Table I, it can be observed that average cell sizes of PP/WGRT composites decrease with increasing the SEBS-*g*-MA loading, whereas the corresponding cell densities and relative densities increase. The addition of compatiblizer (SEBS-*g*-MA) leads to the chemical interactions between the phenolic hydroxyl groups in WGRT and maleic anhydride groups in SEBS-*g*-MA in which an interphase between the dispersed phase (WGRT) and the polymer matrix (PP) was formed.[21] Therefore, the addition of WGRT to PP without SEBS-*g*-MA leads to a poor surface adhesion between PP and WGRT. The poor surface adhesion provides a channel through which CO_2 can quickly escape from the composites.[19,20] However, the presence of SEBS-*g*-MA decreases the possibility so as to facilitate cell nucleation and growth. In addition, the presence of SEBS-*g*-MA increases the viscosity of PP/WGRT composites[22] so as to obstruct cell nucleation and growth. The results is that the increase of viscosity is found to be the more important factor determining cell size of the composites than that of compatibility, namely cell sizes decrease and the corresponding cell densities increase. The relative densities of PP/WGRT composite with the higher SEBS-*g*-MA loading increase due to the formation of the thicker cell wall.

Effect of Processing Condition on Microcellular Structure.

Saturation Temperature: It has been reported that saturation temperature is an important processing parameter to control the foam structure of microcellular polymer.[23-26] Figure 4 and Figure 5 show the foam structures of pure PP and PP/WGRT=70/30 composite obtained at different saturation temperatures for a given saturation pressure of 18 MPa and a given saturation time of 3 h. Foam structure of pure PP and PP/WGRT=70/30 composite exhibits similar tendency with saturation temperature and the foam characteristics for samples can be seen in Table II. From Table II, it can be found that the average cell sizes obtained at 120, 150 and 160 °C slightly increase and are significantly smaller than that at 165 °C. The corresponding cell density first increases until 150 °C then decreases from 150 to 165 °C. Moreover, the relative densities are the lowest due to the formation of the thinnest cell wall when the saturation temperature was at 165 °C.

When the saturation temperature is close to its lower limit for foaming, the $scCO_2$ is expected to dissolve in and diffuses through the amorphous phase rather than the crystalline regions. Therefore, both cell nucleation and cell growth take place mainly in the amorphous regions and the crystalline regions remain virtually intact. Meanwhile, since the

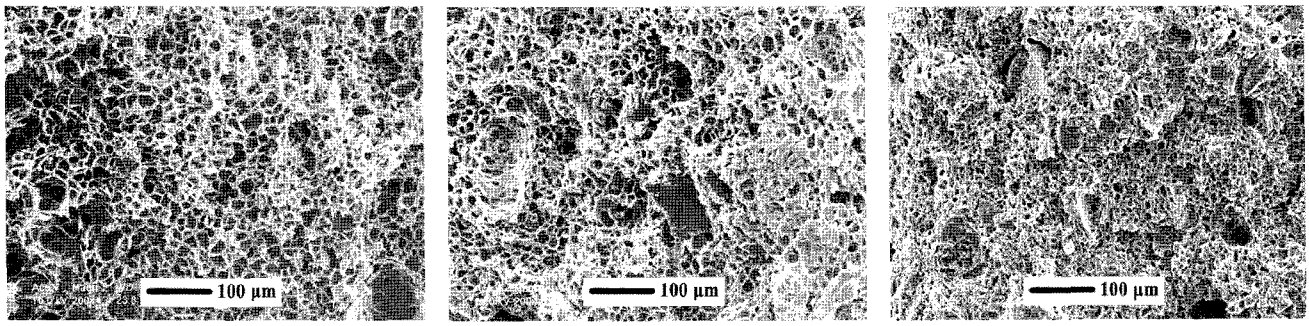

(a) (b) (c)

Figure 3. Effect of SEBS-*g*-MA loading on microcellular structure of PP/WGRT blends foaming at 18 MPa, 165 °C: (a) PP/WGRT/SEBS-*g*-MA=60/40/0; (b) PP/WGRT/ SEBS-*g*-MA=60/40/5; (c) PP/WGRT/SEBS-*g*-MA=60/40/20 (SEM microphotograph).

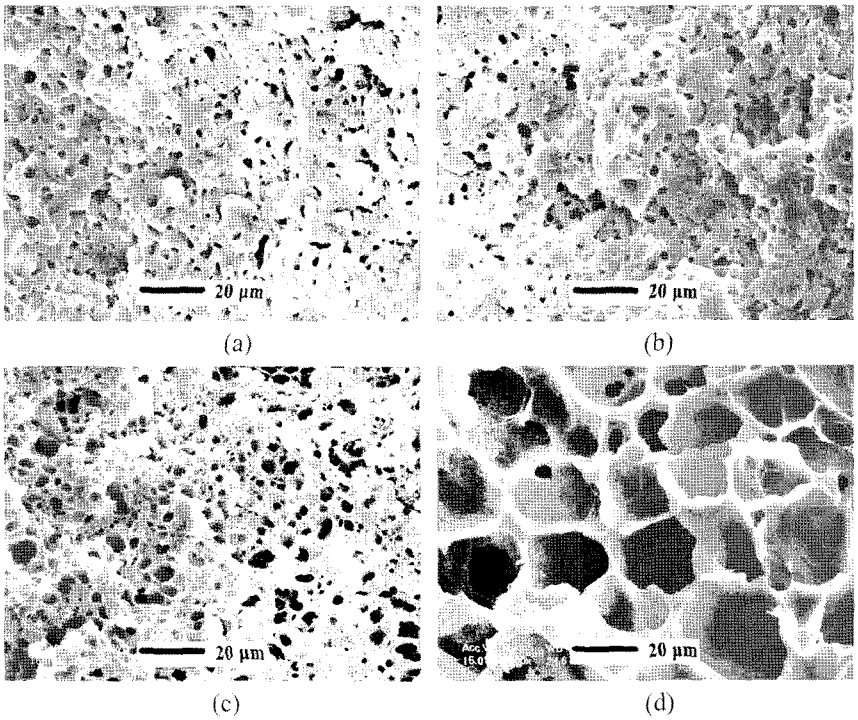

Figure 4. Effect of saturation temperature on microcellular structure of pure PP foaming at 18MPa for 3 h: (a) 120 °C; (b) 150 °C; (c) 160 °C; (d) 165 °C (SEM microphotograph).

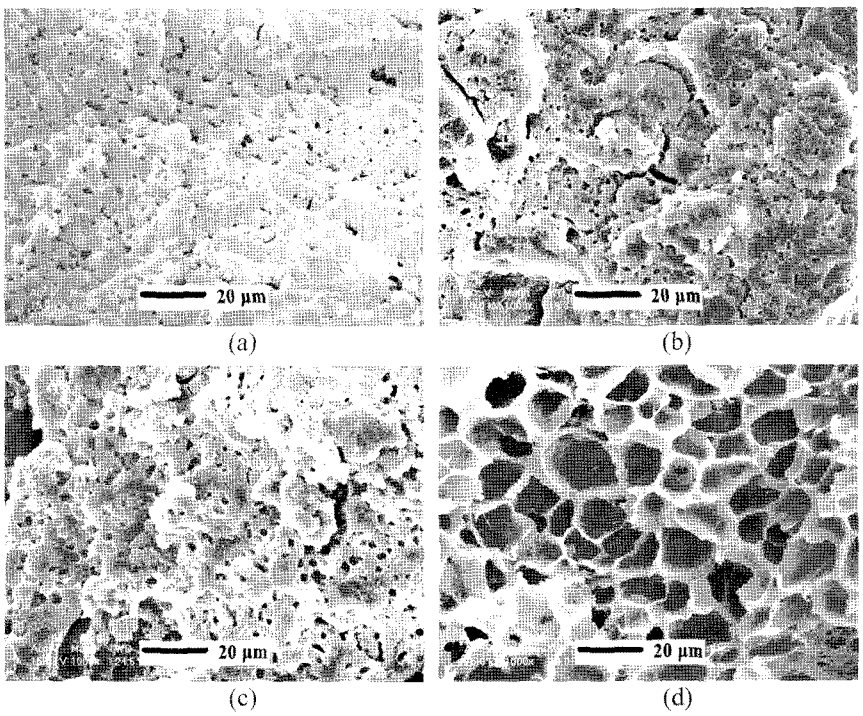

Figure 5. Effect of saturation temperature on microcellular structure of PP/WGRT=70/30 blend foaming at 18 MPa for 3 h: (a) 120 °C; (b) 150 °C; (c) 160 °C; (d) 165 °C (SEM microphotograph).

stiffness of the PP is the higher, its deformability and foamability are the weaker. As a result, the cell sizes are expected to be the smaller and the tested temperature is too low to detect any significant variations in cell sizes. This was the

case when the saturation temperature was at 120, 150 and 160 °C. Doroudiani[27] obtained similar results through foaming experiments by rapid heating. It is noticeable that the corresponding cell densities slightly increase until 150 °C then decrease from 150 to 165 °C. The reason for a maximum in cell densities is that both cell nucleation and cell growth rates increase with saturation temperature and both phenomena compete for the gas available in the system. This leads to a maximum at some optimum temperature.

When the saturation temperature is close to its upper limit for foaming, the crystalline phase can be partly or totally disrupted. Therefore $scCO_2$ is expected to dissolve in and diffuse through both the amorphous phase and the disrupted part of the crystalline phase. Moreover, the deformability and foamability of PP are improved, so conditions become more favorable to foam for PP and grow bigger for the cells. All these facts explain the foam structure obtained at 165 °C. A closer look at it shows that there are many small holes on the cell walls. This should be ascribed that the saturation temperature of 165 °C was actually very close to its upper limit for foaming, 166 °C. The melt strength of the PP under this condition was so weak that dissolved CO_2 could penetrate through the cell walls, creating these tiny holes during the depressurization stage.

Saturation Pressure: Saturation pressure is another effective controlling parameter for microcellular foam.[7] Figure 6 shows the effect of the saturation pressure on the foam structures of pure PP and PP/WGRT=70/30 composite obtained at a given saturation temperature of 165 °C and for a given saturation time of 3 h. Foam structure of pure PP and PP/

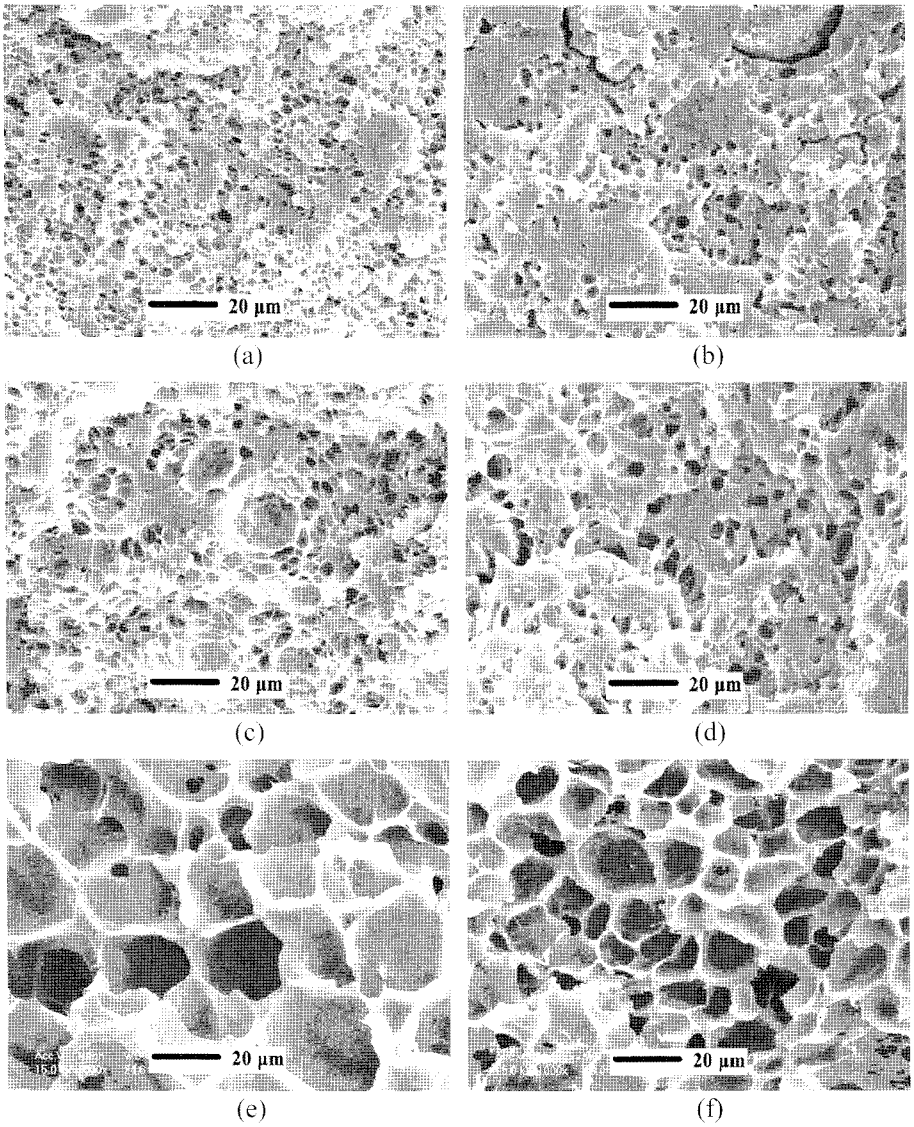

Figure 6. Effect of saturation pressure on microcellular structure of PP/WGRT blends foaming at 165 °C for 3 h: (a) PP/WGRT=100/0 (10 MPa); (b) PP/WGRT=70/30 (10 MPa); (c) PP/WGRT=100/0 (14 MPa); (d) PP/WGRT=70/30 (14 MPa); (e) PP/WGRT=100/0 (18 MPa); (f) PP/WGRT=70/30 (18 MPa) (SEM microphotograph).

WGRT=70/30 composite exhibits similar tendency with saturation pressure and the foam characteristics for samples can be seen in Table II. For Table II, it can be found that average cell sizes of PP/WGRT composites increase with increasing the saturation pressure, whereas the corresponding cell densities and relative densities decrease.

Increasing saturation pressure amounts to increasing saturation temperature. When the saturation pressure is the lower, the extent of the CO_2 induced-melting temperature depression is the smaller, namely the dissolved amount of CO_2 in PP is the lesser. Thus the PP is the stiffer and its deformability and foamability are the smaller. When saturation pressure is the higher, both the CO_2 induced-melting temperature depression and the dissolved amount of CO_2 in PP become very important. As a result, the melt strength of the PP is the weaker, namely its deformability and foamability are the more obvious. Thereby the appearance of the larger cell sizes and the thinner cell walls brings on the reduced cell densities and relative densities with the increase of saturation pressure.

Conclusions

Polypropylene (PP)/waste ground rubber tire powder (WGRT) microcellular composites were successfully prepared with $scCO_2$ pressure-quench process. The microcellular structure of PP/WGRT composites was dependent on the blend composition and processing condition. The higher WGRT and SEBS-g-MA content resulted in the smaller cell sizes, higher cell densities and relative densities, whereas the higher saturation pressure led to the larger cell sizes, lower cell density and relative densities. As for saturation temperature, cell sizes increased and relative densities decreased with the saturation temperature, whereas cell densities first increased then decreased. All phenomena should be ascribed that the variation of blend composition and operation condition resulted in the change of the dissolved amount of CO_2 in PP, the diffusivity of CO_2 within PP and the diffused rate of CO_2 from PP.

Acknowledgements. The authors are grateful to the support from the BK21 program in South Korea.

References

(1) K. W. Suh, C. P. Park, M. J. Maurer, M. H. Tusim, R. D. Genova, R. Broos, and P. S. Daniel, *Adv. Mater.*, **12**, 1779 (2000).
(2) V. Kumar, *Cell. Polym.*, **12**, 207 (1993).
(3) D. L. Tomasko, H. Li, D. Liu, and X. Han, *Ind. Eng. Chem. Res.*, **42**, 6431 (2003).
(4) D. I. Collias and D. G. Baird, *Polymer*, **35**, 3978 (1994).
(5) B. Krause, H. J. P. Sijbesma, P. Münüklü, N. F. A. Van der Vegt, and M. Wessling, *Macromolecules*, **34**, 8792 (2001).
(6) S. Doroudiani, C. B. Park, and M. T. Kortschot, *Polym. Eng. Sci.*, **36**, 2645 (1999).
(7) S. K. Goel and E. J. Beckman, *Polym. Eng. Sci.*, **34**, 1137 (1994).
(8) J. E. Martini-Vvedensky, N. P. Suh, and F. A.Waldman, U.S. Patent 4,473,665 (1984).
(9) J. S. Chiou, J. W. Barlow, and D. R. Paul, *J. Appl. Polym. Sci.*, **30**, 2633 (1985).
(10) H. E. Naguib, C. B. Park, U. Panzer, and N. Reichelt, *Polym. Eng. Sci.*, **42**, 1481 (2002).
(11) N. C.Nayak and D. K.Tirpathy, *J. Mat. Sci.*, **37**, 1347 (2002).
(12) J. Z. Liang and R. K. Y. Li, *J. Appl. Polym. Sci.*, **77**, 409 (2000).
(13) G. K. Jana and C. K. Das, *Macromol. Res.*, **13**, 30 (2005).
(14) C. K. Kum, Y. T. Sung, and Y. S. Kim, *et al.*, *Macromol. Res.*, **15**, 308 (2007).
(15) S. H. Lee, B. Maridass, and J. K. Kim, *J. Appl. Polym. Sci.*, **106**, 3209 (2007).
(16) D. I. Collias, D. G. Baird, and R. J. M. Borggreve, *Polymer*, **35**, 3978 (1994).
(17) L. M. Matuana, C. B. Park, and J. J. Balatinecz, *Polym. Eng. Sci.*, **38**, 1862 (1998).
(18) E. Lievana, *Recycling of Ground Tyre Rubber and Polyolefin Wastes by Producing Thermoplastic Elastomers*, Doctoral dissertation, Argentina, 2005, Chapter 5, p. 99.
(19) L. M. Matuana, C. B. Park, and J. J. Balatinecz, *Cellul. Polym.* **17**, 1 (1998).
(20) L. M. Matuana, C. B. Park, and J. J. Balatinecz, *Polym. Eng. Sci.*, **37**, 1137 (1997).
(21) Z. X. Zhang, V. Sridhar, and J. K. Kim, *Polymer Composites*, 2007 (Accepted).
(22) S. H. Lee, *Study on Dynamic Reaction on Olefinic Thermoplastic Vulcanizate Using Waste Ground Rubber Tire Powder*, Doctoral dissertation, South Korea, 2006, Chapter 4, p.186.
(23) K. A. Arora, A. J. Lesser, and T. J. McCarthy, *Macromolecules*, **31**, 4614 (1998).
(24) C. M. Stafford, T. P. Russell, and T. J. McCarthy, *Macromolecules*, **32**, 7610 (1999).
(25) K. N. Lee, H. J. Lee, and J. H. Kim, *Polym. Int.*, **49**, 712 (2000).
(26) M. T. Liang and C. M. Wang, *Ind. Eng. Chem. Res.*, **39**, 4622 (2000).
(27) S. Doroudiani, C. B. Park, and M. T. Kortschot, *Polym. Eng. Sci.*, **36**, 2645 (1996).